Meson Resonance Production in $\pi^+ - d$ Interactions at 1.23 BeV/c*

ROBERT KRAEMER, LEON MADANSKY,** MOSLEY MEER,† MIRKO NUSSBAUM,†† AIHUD PEVSNER,§ CLARENCE RICHARDSON,‡ RICHARD STRAND,‡ AND RICHARD ZDANIS
Department of Physics, Johns Hopkins University, Baltimore, Maryland

THOMAS FIELDS‡‡ AND STEPHEN ORENSTEIN
Department of Physics, Northwestern University, Evanston, Illinois

AND

TIMOTHY TOOHIG
Research Institute for the Natural Sciences, Woodstock College, Woodstock, Maryland

(Received 8 June 1964)

A report is made of the study of production and decay properties of the η^0, ω^0, ρ^0, and π^0 mesons produced in $\pi^+ - d$ collisions at 1.23 BeV/c in the Berkeley 72-in. bubble chamber. The production processes are analyzed in terms of π^+-neutron interactions through the use of an impulse model. A clear enhancement due to the $N_{1/2}$* (1688) resonance is observed in the π^0 (charge exchange) production cross section. The mass of the η^0 meson is found to be ($m_{\eta^0}=552\pm3$ MeV) with a branching ratio of $(\eta^0 \to \text{all neutrals})/(\eta^0 \to \pi^+\pi^-\pi^0)=3.6\pm0.8$, and the partial width $\Gamma(N_{1/2}^*(1688) \to p+\eta^0)<2$ MeV. The central value of the ω^0-meson peak is found to be ($m_{\omega^0}=781\pm2$ MeV), with a branching ratio $(\omega^0 \to \text{all neutrals})/(\omega^0 \to \pi^+\pi^-\pi^0)=8\pm3\%$, and an upper limit of 5% for decay into two charged pions. The production of the ω^0 is found to be inconsistent with the single-vector-meson exchange model.

INTRODUCTION

THIS paper is a report on multipion resonance production as observed in the interaction of 1.23-BeV/c positive pions with deuterium in the Alvarez 72-in. bubble chamber. Much of the data concerns the η^0 meson,[1] and the ω^0 meson,[2] and preliminary results have been previously reported.[3–5] In addition, we have observed π^0 production (charge-exchange scattering) and ρ^0 production. All of these neutral meson systems (x^0) were produced by the same basic reaction:

$$\pi^+ + n \to x^0 + p. \quad (1)$$

The motivation for an experiment of this type is, of course, to study the production and decay properties of these new neutral meson systems. For this purpose, the above reaction is very convenient from an experimental viewpoint, having no other neutral particle in the final state except the system x^0.

Recent progress toward a clearer understanding of both meson and baryon states in terms of the SU_3 symmetry of the strong interactions[6,7] appears very promising. For our present purposes, we only note that the mesons[8] seem to form a pseudoscalar octet (π,K,η) and a vector octet (ρ,K^*,ω/ϕ). The quantum numbers of these mesons are quite well established, so that the present goal for experiments is to obtain data on their production and decay properties in order to elucidate the dynamics of such processes.

The target neutron was provided by the bubble chamber deuterium, and the events which were used in the actual analysis were of the type

$$\pi^+ + d \to p + p + x^0, \quad (2)$$

where both protons left measurable tracks, and at least one of the protons stopped in the chamber. As long as the decay products of the neutral meson system x^0 include no more than one neutral particle, the reaction is kinematically overdetermined, so that a discrimination among various event identification hypotheses may be accomplished using goodness of fit criteria (χ squared). This procedure also yields fitted values for kinematic quantities such as invariant masses, using only energy-momentum conservation.

In order to interpret the observed events, Eq. (2), in terms of pion-neutron reactions, Eq. (1), we have used an impulse approximation model. The basic assumption of the model is that the proton of the deuteron acts as

* Supported by the U. S. Air Force Office of Scientific Research, the National Science Foundation, the U. S. Office of Naval Research. AFOSR 234-63, and the U. S. Atomic Energy Commission Computation Center.
** Supported by the U. S. Atomic Energy Commission.
† Present address: Purdue University, Lafayette, Indiana.
†† Present address: Columbia University, New York.
§ John S. Guggenheim Foundation Fellow, 1963–1964. Fulbright-Hayes Research Fellow, 1963–1964.
‡ Present address: Brookhaven National Laboratory.
‡‡ Also at Argonne National Laboratory.
[1] A. Pevsner, R. Kraemer, M. Nussbaum, C. Richardson, P. Schlein *et al.*, Phys. Rev. Letters **7**, 421 (1961).
[2] B. Maglić, L. Alvarez, A. Rosenfeld, and M. L. Stevenson, Phys. Rev. Letters **7**, 179 (1961).
[3] T. Toohig, R. Kraemer, L. Madansky, M. Meer, M. Nussbaum *et al.*, in *Proceedings of The 1962 Annual International Conference on High Energy Physics at CERN*, edited by J. Prentki (CERN, Geneva, 1962), p. 103.
[4] M. Meer, R. Strand, R. Kraemer, L. Madansky, M. Nussbaum *et al.*, in *Proceedings of the 1962 Annual International Conference on High Energy Physics at CERN*, edited by J. Prentki (CERN, Geneva, 1962), p. 107.
[5] T. Fields, S. Orenstein, R. Kraemer, L. Madansky, M. Meer *et al.*, in *Proceedings of the Athens Topical Conference on Resonant Particles* (Ohio University Press, Athens, Ohio, 1962), p. 185.
[6] M. Gell-Mann, Phys. Rev. **125**, 1067 (1962) V. Barnes, P. Connolly, D. Crennel, B. Culwick, W. Delaney *et al.*, Phys. Rev. Letters **12**, 204 (1964).
[7] Y. Ne'eman, Nucl. Phys. **26**, 222 (1961).
[8] G. Puppi, Ann. Rev. Nucl. Sci. **13**, 287 (1963).

a spectator, and appears in the final state, Eq. (2), with its momentum unchanged by the collision. In a later section, we discuss this model in detail; here we note that the identification of resonant states and their decay modes does not involve the impulse model.

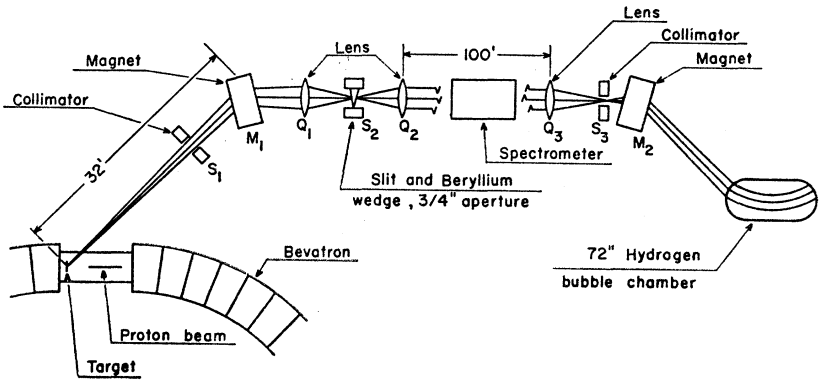

FIG. 1. Schematic layout of the bubble chamber and beam transport system.

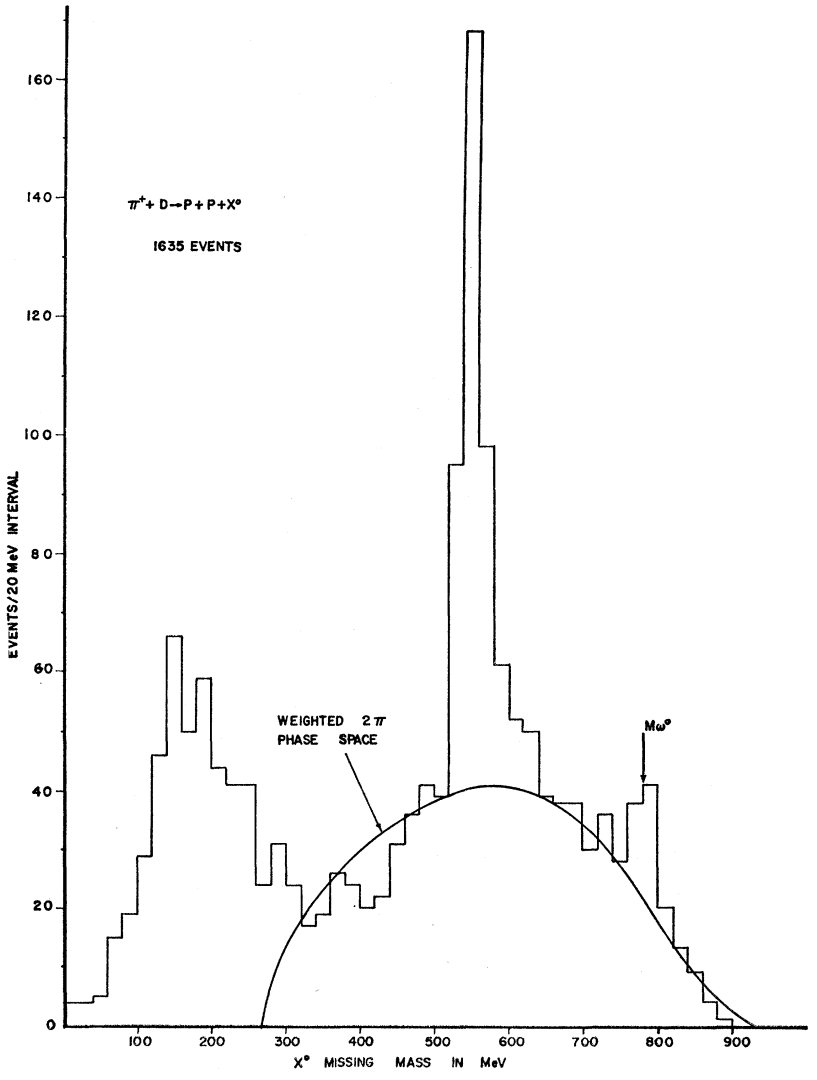

FIG. 2. Missing mass distribution for two-pronged events. The solid curve is two-pion phase space, appropriately averaged over the range of c.m. energies covered in this experiment. It is normalized to the apparent background in the mass region 600–900 MeV.

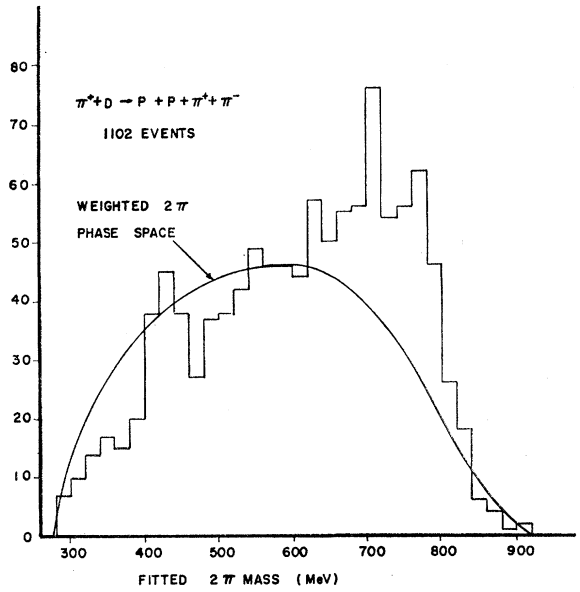

FIG. 3. Invariant mass distribution for $(\pi^+\pi^-)$ final states. The normalization of the phase-space curve is arbitrary.

EXPERIMENTAL ARRANGEMENT

A schematic diagram showing the beam transport system and bubble chamber is given in Fig. 1. The beam transport system was that of Crawford,[9] and yielded a π^+ momentum of 1.232 ± 0.015 BeV/c at the entrance window of the chamber. The quoted error includes both the uncertainty in the central value and the rms spread of momenta contained in the beam, and was verified by curvature measurements and kinematic fitting on typical events in the bubble chamber. The mass analysis provided by the beam system resulted in a total contamination of $(5\pm2)\%$ of protons, muons, and positrons, as determined by delta ray analysis and kinematic analysis.[10] A contamination of about 1% hydrogen was present in the chamber deuterium, but the restriction of the data to events with two visible protons in the final state eliminated interactions on hydrogen.

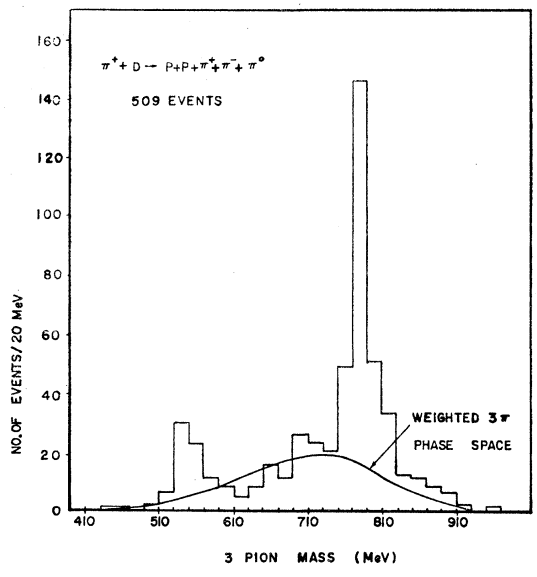

FIG. 4. Invariant mass distribution for $(\pi^+\pi^-\pi^0)$ final states. The normalization of the phase-space curve is arbitrary.

DATA REDUCTION

A total of 2.6×10^7 cm of track in a selected fiducial volume was double-scanned for events having either of two topologies:

$$\pi^+ + d \rightarrow p + p + \text{neutrals}, \quad \text{(two outgoing prongs)}, \quad (3)$$

$$\pi^+ + d \rightarrow p + 3 \text{ charged prongs}, \quad \text{(four outgoing prongs)}. \quad (4)$$

The scanning for the first topology, two-pronged events, included a criterion that the projected curvature of the higher momentum track corresponds to less than 1 BeV/c, in order to permit visual identification of the outgoing prongs as protons by their bubble density. For both topologies it was required that at least one of the protons stop in the bubble chamber. This stopping proton, or the shorter of the two in events in which two protons stopped, was assumed to be the spectator proton in the impulse model, as discussed below. Appropriate cutoffs on minimum track lengths were used, and all events of both categories were checked on the scanning table by physicists. The scanning efficiency per single scan was about 85% for two-pronged events and 95% for four-pronged events, as deduced from the second scan results. Measurement of the events was

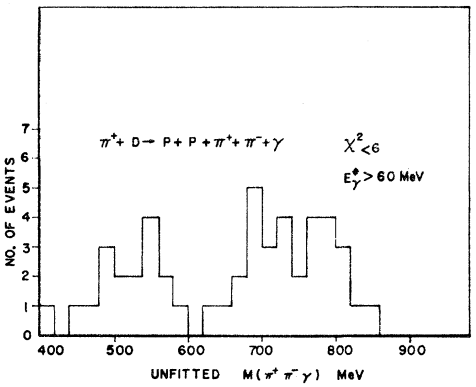

FIG. 5. Invariant mass distribution for final states which fitted $(\pi^+\pi^-\gamma)$.

[9] S. Wolf, N. Schmitz, L. Lloyd, W. Lasker, F. Crawford *et al.*, Rev. Mod. Phys. 33, 439 (1961).

[10] J. B. Shafer, F. Crawford, R. Hubbard, M. L. Stevenson, M. Block *et al.*, Phys. Rev. 130, 2077 (1963).

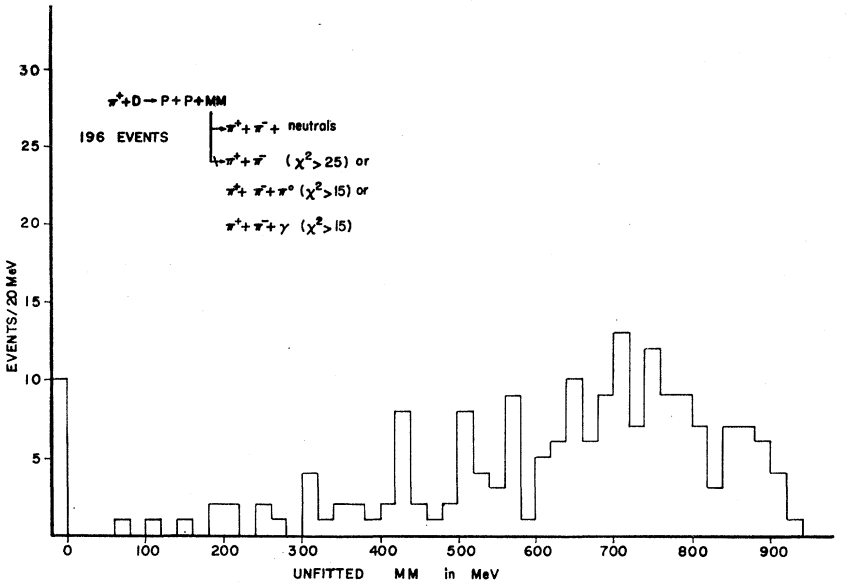

FIG. 6. Effective mass distribution for four-pronged events which fit none of the hypotheses.

carried out using digitized measuring machines of standard design. Track reconstruction and kinematic analyses were carried out using the standard sequence of Berkeley computer programs.[11] Two-pronged events were tried for fits to the following hypotheses:

$$\pi^+ d \rightarrow p+p+\pi^0, \quad (3a)$$
$$\rightarrow p+p+\eta^0, \quad (3b)$$
$$\rightarrow p+p+\omega^0, \quad (3c)$$
$$\rightarrow p+K^++\Lambda^0, \quad (3d)$$
$$\rightarrow p+K^++\Sigma^0, \quad (3e)$$
$$\rightarrow p+\pi^++n. \quad (3f)$$

Also, for each event, an invariant missing mass was calculated, according to the scheme:

$$\pi^++d \rightarrow p+p+\text{missing mass}. \quad (3g)$$

Figure 2 shows a histogram of the missing mass distribution from all two-pronged events for which the spectator momentum was less than 300 MeV/c and for which the hypothesis (3f) gave an unacceptable fit. Peaks due to reactions (3a) and (3b) are clearly visible, in addition to the continuum arising from events with two or more neutral pions in the final state.

The four-pronged events, Eq. (4), were fitted for the hypotheses:

$$\pi^++d \rightarrow p+p+\pi^++\pi^-, \quad (4a)$$
$$\rightarrow p+p+\pi^++\pi^-+\pi^0, \quad (4b)$$
$$\rightarrow p+\pi^++\pi^++\pi^-+n, \quad (4c)$$
$$\rightarrow p+p+\pi^++\pi^-+\gamma. \quad (4d)$$

The appropriate permutations of π^+ and proton mass were used in the fitting process, in order to guard against misidentification in the scanning process. The bubble density was checked for most events and was useful in some cases for ruling out one or more fits for ambiguous events. Also, for each event, the invariant missing mass for the following reaction was computed:

$$\pi^++d \rightarrow p+p+\pi^++\pi^-+\text{missing mass}. \quad (4e)$$

Figure 3 is a histogram of the invariant mass of the $(\pi^+\pi^-)$ system for those events which fit reaction (4a) with $\chi^2 < 25$, which did not fit reaction (4b), and which yielded a missing mass of less than 100 MeV in reaction (4e) (to eliminate imprecise events).

Figure 4 shows a histogram of the invariant mass of the $(\pi^+\pi^-\pi^0)$ system for those events which fit reaction (4b) with $\chi^2 < 6$, and which gave a χ^2 for reaction (4a) of greater than 25. Additionally, it was required that the magnitude of the error in the missing mass of Eq. (4e) be less than 100 MeV, to eliminate inaccurate events. The η^0 and ω^0 peaks are prominent, amounting to about 11% and 15%, respectively, of the total number of events shown.

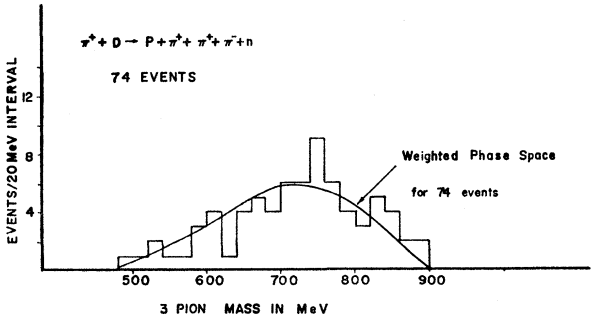

FIG. 7. Invariant mass distribution for $(\pi^+\pi^+\pi^-)$ final states, reaction (4c).

[11] A. Rosenfeld and W. Humphrey, Ann. Rev. Nucl. Sci. 13, 103 (1963).

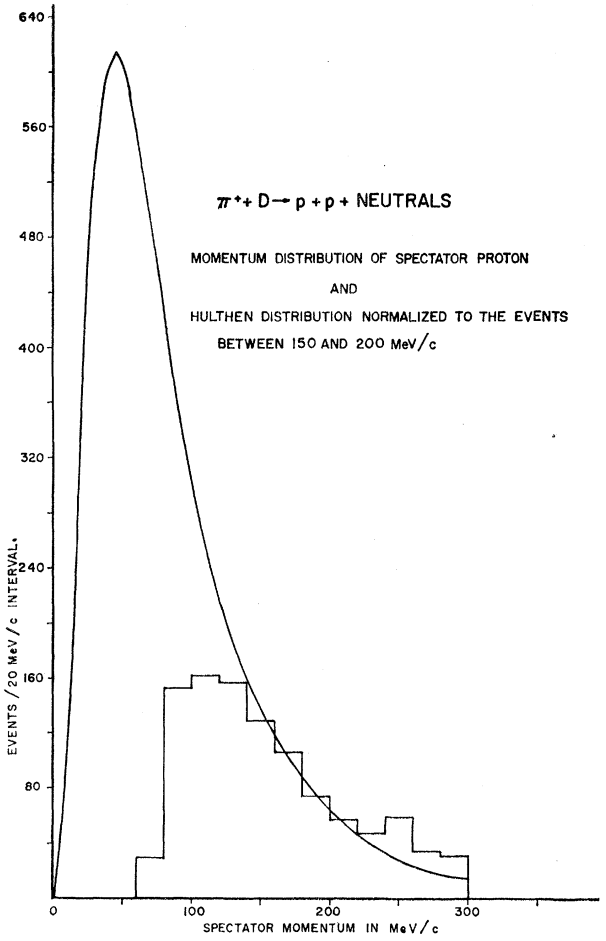

FIG. 8. Distribution in momentum of the lower energy proton for two-pronged events, Eq. (3). The solid curve is the Hulthén distribution, Eq. (6), normalized to fit the data over the momentum range 150–200 MeV/c. The experimental falloff at lower momenta is due to scanning bias against very short tracks.

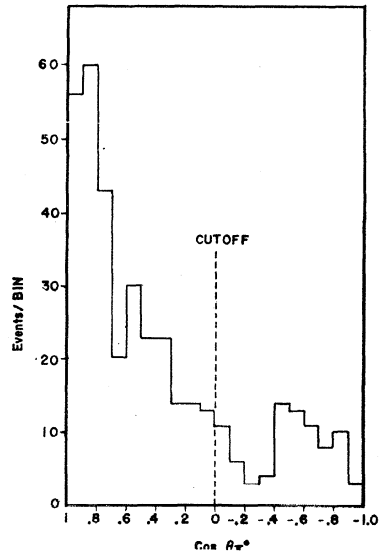

FIG. 9. C.m. angular distribution of neutral pions in charge-exchange scattering. Note that these data and most of the other production data of this experiment represent an average over c.m. total energies from about 1600 MeV. The line marked cutoff shows the maximum angle corresponding to the 1 BeV/c cutoff on recoil proton momentum, for a stationary target neutron.

Figure 5 shows the invariant mass distribution of the $(\pi^+\pi^-\gamma)$ system for events which fit reaction (4d). Figure 6 shows the distribution of effective mass for four-pronged events which fit none of the reactions (4a) through (4d). Finally, Fig. 7 is an invariant mass distribution of the $(\pi^+\pi^+\pi^-)$ system for events which fit reaction (4c). In each case, the χ^2 criteria are shown on the figure.

IMPULSE MODEL

In order to use data from the invariant mass distribution to study production processes for the various mesons, we have made use of an impulse approximation model. The basic assumption is that the incoming positive pion interacts only with the neutron, leaving the spectator proton to recoil with a momentum distribution given by the square of the Fourier transform of the Hulthén wave function[12,13]:

$$P(p)dp = 4\pi\phi^2(p)p^2dp \tag{5}$$

$$= \frac{4}{\pi}\left[\frac{\alpha\beta(\alpha+\beta)}{(\alpha-\beta)^2}\right]\left[\frac{1}{\alpha^2+p^2}-\frac{1}{\beta^2+p^2}\right]^2 p^2dp, \tag{6}$$

where $\alpha=(\mu\epsilon)^{1/2}=45.5$ MeV, μ=nucleon mass, ϵ=deuteron binding energy, and $\beta=7\alpha$, $c=1$. The maximum of this distribution occurs at a nucleon momentum of 50 MeV/c, while the probability for $p<300$ MeV/c is 0.99.

The approximate validity of such a model has been shown in several experiments,[14,15] although a clear

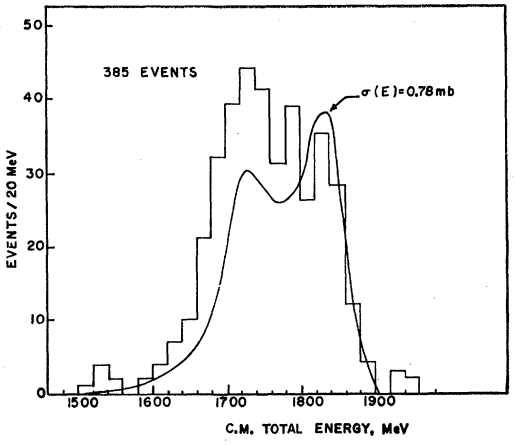

FIG. 10. Distribution in total c.m. energy for charge-exchange events. The solid curve is calculated using Eq. (7), assuming $\sigma(E)$ constant and a spectator projected range cutoff of 2.0 mm.

[12] L. Hulthén, Arkiv. Mat. Astron. Fysik **35A**, No. 25 (1948).
[13] L. Hulthén and M. Sugawara, in *Handbuch der Physik*, edited by S. Flügge (Springer-Verlag, Berlin 1957), Vol. 39, p. 1.
[14] W. Chinowsky, G. Goldhaber, W. Lee, T. O'Halloran, T. Stubbs *et al.*, in *Proceedings of the Tenth Annual Rochester Conference on High-Energy Physics, 1960* (Interscience Publishers, Inc., New York, 1960), p. 451.
[15] R. Kraemer, M. Nussbaum, L. Madansky, and A. Pevsner, in *Proceedings of the 1962 Annual International Conference on High-Energy Physics at CERN*, edited by J. Prentki (CERN, Geneva, 1962), p. 273.

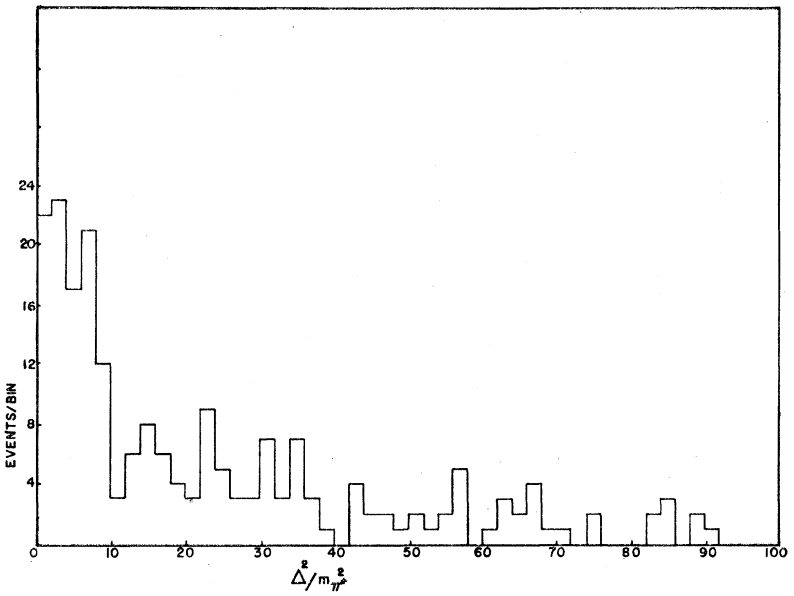

FIG. 11. Distribution in four-momentum transfer to the target nucleon for charge-exchange events.

understanding of the n-p interaction at short distances and its effect upon the high-momentum components of the deuteron wave function has not yet been reached.

In the analysis of the data, only those events were included where the momentum of the spectator proton, in the sense of the impulse model, was less than 300 MeV/c. This restricts the sample to those events for which both experimental and theoretical investigation have indicated the validity of the Hulthén wave function. It also minimizes the contribution to the counting rate from "rescattering" events, in which a primary reaction with the neutron is followed by a scattering from the spectator proton.

For those events with two final-state protons of momenta less than 300 MeV/c, we have taken the lower energy one to be the spectator; this should not introduce a large error, since the number of such events is only a few percent of the total. Such an error is most serious for cases wherein the recoil proton in Eq. (1) would emerge with low energy in the laboratory system, since the Pauli exclusion principle and final-state interaction between the two protons may then have appreciable effects.

A gross experimental check upon the validity of the impulse model is given in Fig. 8. One sees that the observed momentum distribution for spectator protons in two-pronged events seems to be fairly consistent with the Hulthén distribution, taking account of the scanning bias against short-proton prongs with momentum less than about 120 MeV/c.

In order to make a more detailed comparison of our results with the predictions of such an impulse model, it is necessary to take account of two effects which logically form a part of the model. These are: first, the c.m. energy of the pion-neutron collision varies over a considerable range, depending on the vector momentum of the struck neutron; second, the relative velocity of the pion and neutron and thus the effective current of the incident pion wave also depend on the neutron vector momentum. Taking account of these purely kinematic effects, we have expressed the expected counting rate in the form

$$\frac{dn}{dE}=K\sigma_{\pi n}(E)\int v_{\pi n}(E,p)\,|P(p)|^2\epsilon(E,p)J(E,p)dp\,, \quad (7)$$

where the independent variables are E, the total c.m. energy of the pion-neutron system, and p, the magnitude of the spectator 3-momentum. The other pertinent quantities are: σ, the pion-neutron interaction cross section; v, the relative velocity of the pion and neutron; P, the momentum probability defined in Eq. (6); $\epsilon(E,p)$, the scanning efficiency for finding the spectator proton track; K, a normalization constant; and finally J, the Jacobian corresponding to the use of the independent variables E and p. We have numerically evaluated this integral on a digital computer, and have used the resulting curve of expected counting rate versus π-n c.m. energy to measure the factor $\sigma(E)$ for the reaction being studied. The correctness of the cross sections so obtained should thus provide a more precise test of the validity of the impulse model than does the observed spectator momentum distribution.

Three further remarks should be made at this point. The first is that the unstable target formulation of Chew and Low[16] includes the present model as a special case. The second is that the target neutron is not on its mass shell, so that one makes a further approximation in identifying $\sigma(E)$ as a physical cross section. Finally, the impulse model is necessary for the present experi-

[16] G. Chew and F. Low, Phys. Rev. **113**, 1640 (1959).

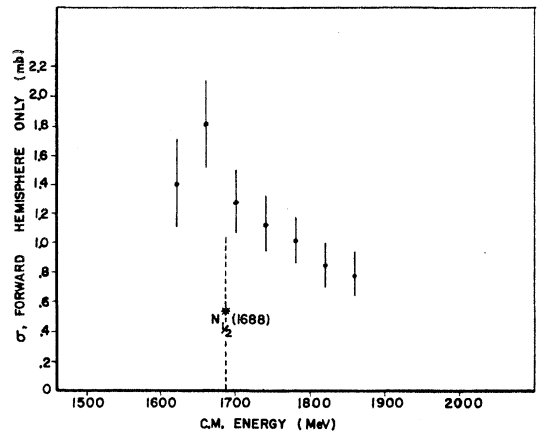

FIG. 12. Charge exchange cross section versus c.m. energy, as deduced using the impulse model.

ment only in studying production processes; the analysis of invariant mass distributions and of decay processes of resonant states does not involve the impulse model.

NEUTRAL PION RESULTS

Figure 2 shows a broad peak in the mass region below 300 MeV, which is due to neutral pions from charge-exchange scattering:

$$\pi^+ + n \rightarrow \pi^0 + p. \tag{8}$$

Using the impulse model, the π^0 angular distribution may be calculated in the $(\pi+n)$ c.m. system, and is given in Fig. 9. Similarly, Fig. 10 shows the distribution in c.m. energy for the charge exchange events, and Fig. 11 shows the distribution in 4-momentum transfer to the struck neutron.

Using Eq. (7), we obtain a curve of expected counting rate versus c.m. energy for constant production cross section, as shown on Fig. 10. Taking the ratio of the observed counting rate to that given by the curve, and normalizing to the track length and cutoffs used in the experiment, we obtained the cross section for charge-exchange scattering as shown in Fig. 12. The results seem in reasonable agreement with data from other experiments[17,18] on the reaction which is charge symmetric to (8), and the cross section exhibits a possible enhancement due to the $N_{1/2}^*$ (1688) resonance. Note that this enhancement is rather independent of the projected range cutoff used in calculating the curve of Fig. 10, because the curve is roughly symmetrical about 1790 MeV for any value of the cutoff. This rough symmetry corresponds, of course, to the equal *a priori* probability of upstream or downstream motion of the initial state neutron. Within the accuracy of our data, then, the impulse model seems to provide an adequate description of the production of neutral pions via charge-exchange scattering.

η MESON RESULTS

The presence of the η meson can be seen in the mass distributions given in Figs. 2, 4, and 6 above. These figures represent the respective decay modes:

$$\eta^0 \rightarrow \text{neutral particles},$$
$$\eta^0 \rightarrow \pi^+ + \pi^- + \pi^0,$$
$$\eta^0 \rightarrow \pi^+ + \pi^- + \gamma.$$

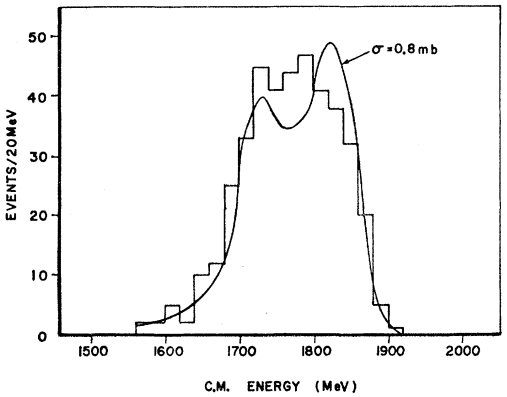

FIG. 13. Distribution in c.m. energy of η^0 production events. The normalization of the solid curve includes a background subtraction.

From these mass distributions, we obtain an η^0 mass of (552 ± 3) MeV, and a full width at half-maximum of about 16 MeV. The latter value is equal within error to the resolution of the system, consistent with the expectation that the η^0 width is much less than 1 MeV.

Making appropriate background and scanning efficiency corrections, we obtain:

$$R(\eta^0 \rightarrow \text{neutrals})/R(\eta^0 \rightarrow \pi^+\pi^-\pi^0) = 3.6\pm0.8, \tag{9}$$

$$R(\eta^0 \rightarrow \pi^+\pi^-\gamma)/R(\eta^0 \rightarrow \pi^+\pi^-\pi^0) = 0.10\pm0.10. \tag{10}$$

These results are in satisfactory agreement with most other published data.[19–24]

The distribution in π-n c.m. energy of the η^0 events is shown in Fig. 13. Comparison with the curve calculated for constant production cross section shows that the cross section for the process

$$\pi^+ + n \rightarrow \eta^0 + p \tag{11}$$

[17] A. Weinberg, A. Brenner, and K. Strauch, Phys. Rev. Letters 8, 70 (1962).
[18] A. Natapoff, University of California, Lawrence Radiation Laboratory Report 11150 (unpublished).
[19] L. Behr, P. Mittner, and P. Musset, Phys. Letters 4, 22 (1963).
[20] F. Crawford, L. Lloyd, and E. Fowler, Phys. Rev. Letters 10, 546 (1963).
[21] M. Chrétien, F. Bulos, H. Crouch, R. Lanou, J. Massimo *et al.*, Phys. Rev. Letters 9, 127 (1962).
[22] C. Alff, D. Berley, D. Colley, N. Gelfand, U. Nauenberg *et al.*, Phys. Rev. Letters 9, 325 (1962).
[23] C. Bacci, G. Penso, G. Salvini, A. Wattenberg, C. Mencuccini *et al.*, Phys. Rev. Letters 11, 37 (1963).
[24] E. Fowler, F. Crawford, L. Lloyd, R. Grossman, and L. Price, Phys. Rev. Letters 10, 110 (1963).

is varying slowly with energy over this region. In particular, the peak corresponding to the $N_{1/2}$* (1688) which appears on Fig. 12, is not in evidence, yielding an upper limit for the partial cross section

$$\pi^+ + n \rightarrow N_{1/2}^*(1688) \rightarrow \eta^0 + p \qquad (12)$$

of about 0.5 mb. This corresponds to a partial width for the $N_{1/2}$*(1688) decay to η+nucleon of less than 2 MeV, quite consistent with the value of 0.5 MeV given by the unitary multiplet coupling scheme of Glashow and Rosenfeld.[25]

The apparent slow variation with energy of the cross section for η^0 production implies that Eq. (7) will reduce to the result that the spectator momentum distribution should be essentially that of the Hulthén wave function. This was found to be the case experimentally; the projected range cutoff which best fit the data was 2.0 mm, corresponding to a fraction 0.69±0.06 of events in which the proton spectator track was undetectably short.

By dividing the counting rate shown on Fig. 13 by the impulse model curve, one obtains a total cross section for η^0 production which is fairly constant over the energy region 1650–1850 MeV with a magnitude of of about (0.8±0.2) mb. Since the threshold for this reaction is at 1490 MeV, the slowly varying cross section provides evidence for a matrix element which is rapidly decreasing with increasing energy.

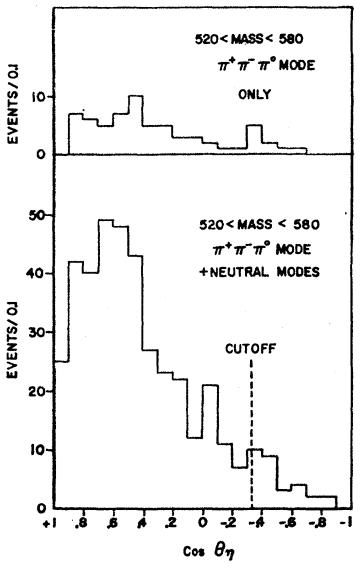

FIG. 14. Angular distribution for η^0 production events.

The c.m. angular distribution for η^0 production is shown in Fig. 14. Although the 1 BeV/c recoil momentum cutoff provides a bias against the large angle events, and impulse model breakdown and scanning efficiency effects provide a bias against the smallest angle events, there seems nevertheless to be evidence for terms in the angular distribution up to $\cos^3\theta$, implying the presence of at least $l=2$ for the η^0. The large front-back asymmetry further implies the dominance of an interference between partial waves of opposite parity.

Figure 15 shows the distribution in 4-momentum transfer to the struck nucleon. The strong interaction conservation laws prevent any presently established meson from acting as the exchanged particle in a peripheral production mechanism.

Finally, the Dalitz plot for events in the η mass region decaying by the $\pi^+\pi^-\pi^0$ mode is given in Fig. 16. As can be seen from Fig. 4, about 20% of the events in the η mass region are actually background events. Puppi[8] has given a summary showing similar data from several experiments. Recently, Crawford[26] has used a background-free sample of $\eta^0 \rightarrow \pi^+\pi^-\pi^0$ decays to study the decay process; in particular, the projection of the Dalitz plot upon the π^0 energy axis can be used to investigate the possible existence of the σ meson state hypothesized by Brown and Singer.[27]

ω MESON RESULTS

The production of the ω^0 meson is evident in the data shown in Fig. 4, yielding a central value for the ω^0 mass of 781±2 MeV. The full width at half-maximum of the experimental peak is 21 MeV, whereas the experimental resolution is about 19 MeV, so that our results imply that the actual width of the ω^0 is less than about 12 MeV. This is quite consistent with the value (9±3) MeV recently reported by Gelfand *et al.*[28]

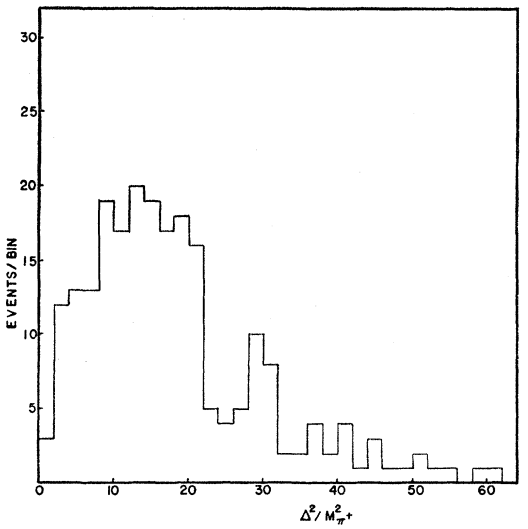

FIG. 15. Distribution in four-momentum transfer to the target nucleon for η^0 production events.

[25] S. Glashow and A. Rosenfeld, Phys. Rev. Letters **10**, 192 (1963).

[26] F. Crawford, R. Grossman, L. Lloyd, L. Price, and E. Fowler, Phys. Rev. Letters **11**, 564 (1963).

[27] L. M. Brown and P. Singer, Phys. Rev. **133**, B812 (1964).

[28] N. Gelfand, D. Miller, M. Nussbaum, J. Ratau, J. Schulz *et al.*, Phys. Rev. Letters **11**, 436 (1963).

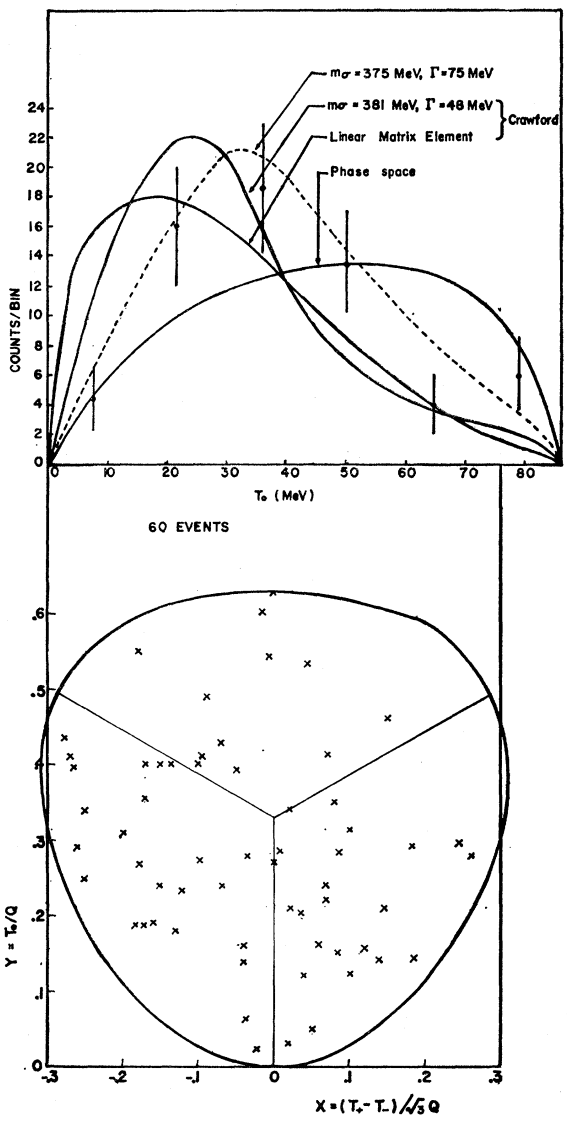

FIG. 16. Dalitz plot for $\eta^0 \rightarrow \pi^+\pi^-\pi^0$. The projection upon the T_0 axis is also shown, and compared with the best fits of Crawford (Ref. 26). A better fit to the present data, using the Brown and Singer model, is shown as a dotted curve.

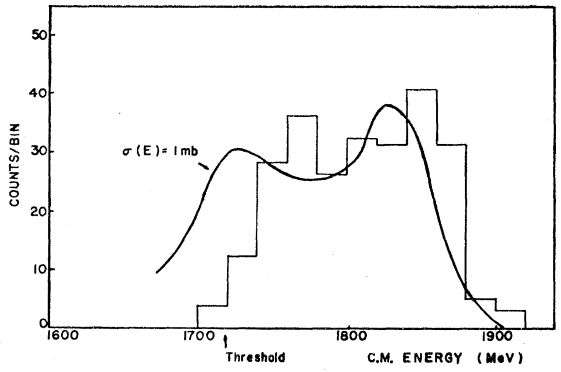

FIG. 17. Distribution in c.m. energy for ω^0 production events.

The mass spectrum of neutral systems shown on Fig. 2 provides evidence for the neutral decay of the ω^0. We obtain the result

$$R(\omega^0 \rightarrow \text{neutral})/R(\omega^0 \rightarrow \pi^+\pi^-\pi^0) = 0.08 \pm 0.03. \quad (13)$$

Some evidence concerning a possible $\pi^+\pi^-$ decay mode of the ω^0 can be derived from Fig. 3. We get an upper limit of 5% for the ω^0 branching ratio into two pions, consistent with other results[29–31] $(1.8_{-0.6}^{+1.2})$ % and $<0.7\%$. On Fig. 17 is shown the distribution in π-n c.m. energy for ω^0 production events. Note that, since threshold is at $M_p + M_{\omega^0} = 1719$ MeV, about one-third of the π-n collisions in this experiment are energetically unable to produce an ω^0. The impulse model then allows the cross sections shown in Fig. 18 to be deduced.

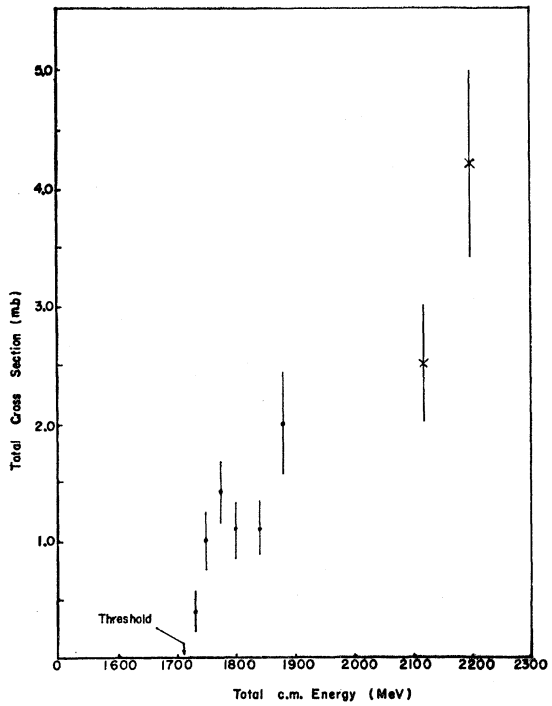

FIG. 18. ω^0 production cross section *versus* c.m. energy. The two highest energy points represent results of Walker *et al.* (Ref. 31).

Also shown are two points obtained by Walker *et al.*[32] from the charge symmetric reaction

$$\pi^- + p \rightarrow \omega^0 + n. \quad (14)$$

Comparison of the two sets of results seems to indicate that the over-all accuracy of the impulse model as we

[29] W. Walker, J. Boyd, A. Erwin, P. Satterblom, M. Thompson, and E. West, Bull. Am. Phys. Soc. **9**, 22 (1964).
[30] G. Lütjens and J. Steinberger, Phys. Rev. Letters **12**, 517 (1964).
[31] W. Fickinger, D. Robinson, and E. Salant, Phys. Rev. Letters **10**, 457, (1963).
[32] W. Walker, E. West, A. Erwin, and R. March, in *Proceedings of the 1962 Annual International Conference on High-Energy Physics at CERN*, edited by J. Prentki (CERN, Geneva, 1962), p. 42 (cross sections increased by 20%—private communication).

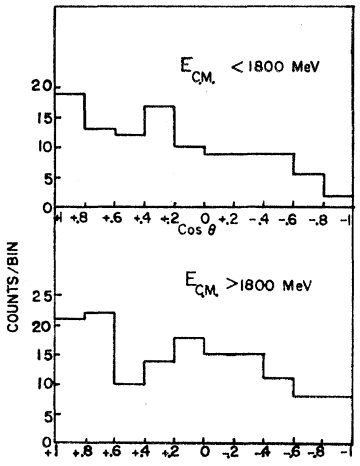

FIG. 19. Angular distribution for ω^0 production events.

have used it for deducing total cross sections for ω^0 production may be as poor as $\pm 30\%$.

The production angular distribution for ω^0 mesons is shown in Fig. 19. Even near threshold, the angular distribution is anisotropic. Figure 20 shows the corresponding distribution in 4-momentum transfer. Further information concerning the production process given in Fig. 21; the distributions are those of the normal to the ω^0 decay plane, measured in the rest frame of the ω^0. The only meson exchange diagram which can contribute to ω^0 production in this experiment is shown in Fig. 22. As discussed by Smith *et al.*[33] in their study of K^* spin alignment, and by others[34,35]; a vector meson exchange process such as Fig. 22 will yield a decay distribution proportional to $\sin^2\beta$. Our results show that this diagram does not dominate the production process. Liu and Singer[36] have shown that

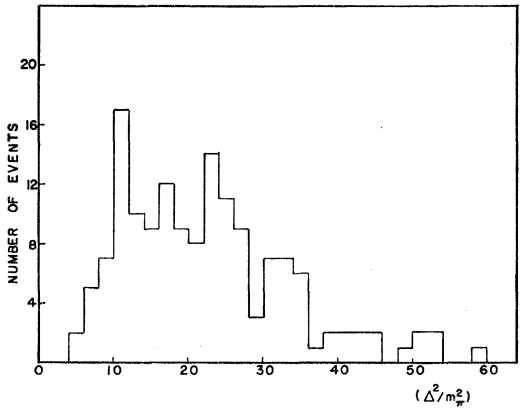

FIG. 20. Distribution in 4-momentum transfer to the target nucleon for ω^0 production events.

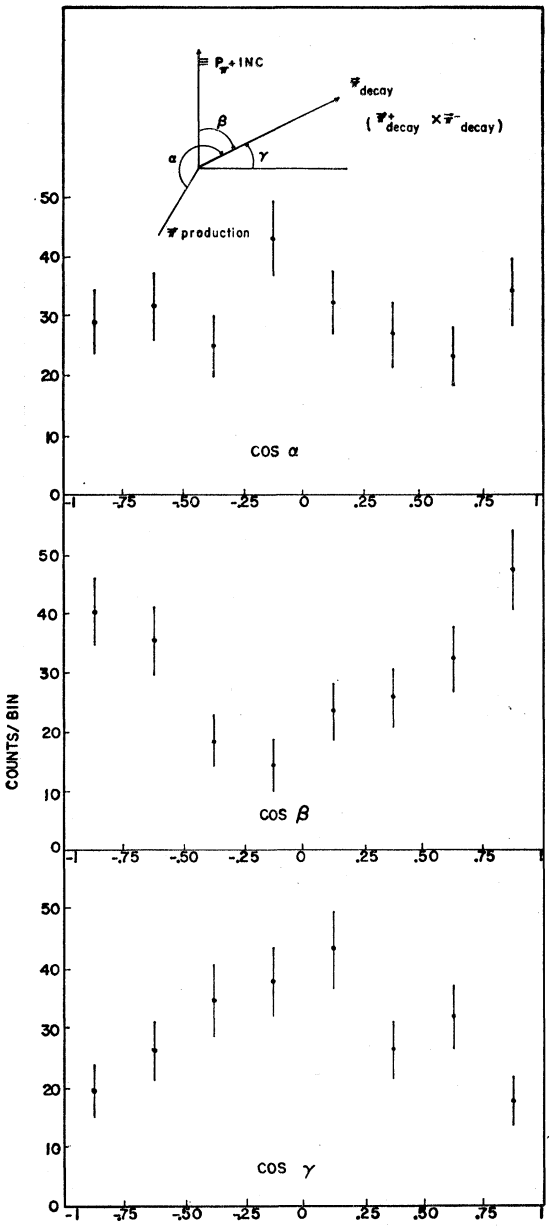

FIG. 21. Decay angular distributions of the normal to the ω^0 decay plane. The angles α, β, and γ are measured in the rest system of the ω^0, and are defined on the figure.

important contributions may be expected from direct emission of the ω^0, i.e., from a nucleon pole diagram.

The Dalitz plot for events in the omega region decaying by the three-pion mode is given in Fig. 23. The radial

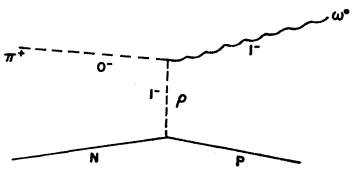

FIG. 22. Diagram for ω^0 production via ρ exchange.

[33] G. A. Smith, J. Schwartz, D. Miller, G. Kalbfleisch, R. Huff *et al.*, Phys. Rev. Letters **10**, 138 (1963).
[34] R. Huff, Phys. Rev. **133**, B1078 (1964).
[35] J. D. Jackson and H. Pilkuhn, CERN Report 8379/TH. 409 (unpublished).
[36] L. Liu and P. Singer, Bull. Am. Phys. Soc. **9**, 63 (1964); Phys. Rev. **135**, B1017 (1964).

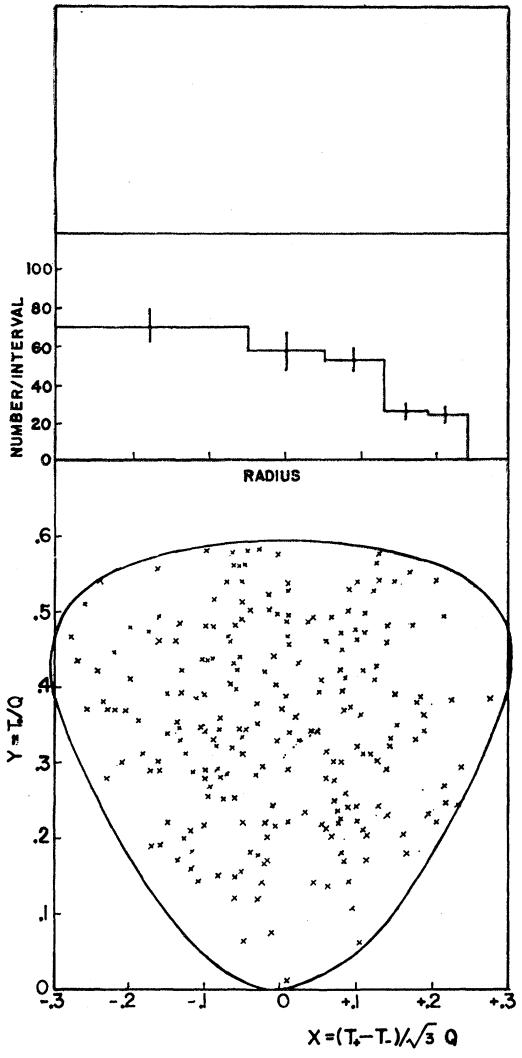

FIG. 23. Dalitz plot for $\omega^0 \to \pi^+\pi^-\pi^0$.

distribution of events, as shown on the Stevenson plot inset in Fig. 23, is characteristic of the accepted 1^- quantum numbers for the omega.

CONCLUDING REMARKS

The events in which the final state contains two pions, Fig. 3, show evidence for ρ-meson production. This evidence becomes much clearer, as expected, if only peripheral collisions are considered. However, the sample still contains a large fraction of $N_{3/2}^*(1238)$ production. Our results seem consistent with previous, more accurate experiments on ρ production,[37] and do not yield any significant new information on the properties of the ρ meson.

The invariant mass distributions shown on Figs. 2–4 provide no clear evidence for meson resonances other than the η^0, ω^0, and ρ^0 in the mass region up to about 850 MeV. A possible exception to this is the bump, which we have previously reported, at about 420 MeV for the $\pi^+\pi^-$ system, as shown on Fig. 3. This may be related to the bump seen by Samios[38] at 390 MeV and may also be related to the σ meson ($T=0$, $J=0$) hypothesized by Brown and Singer.[27] Other anomalies have previously been seen in the isospin zero, low-energy two-pion system, but a clear experimental resolution of the situation seems to demand higher statistical accuracy and the use of a reaction for which $N^*(1238)$ and ρ^0 meson production are not so strong.[39]

ACKNOWLEDGMENTS

The authors would like to thank Dr. Louis Alvarez and the staff of the Lawrence Radiation Laboratory for their cooperation in making the experiment possible. We also would like to thank Professor M. M. Block and Professor L. Brown for helpful discussions, Mrs. Doris Ellis for computer programs, and the scanning and measuring groups at Northwestern and Johns Hopkins Universities.

[37] E. Pickup, D. Robinson, and E. Salant, Phys. Rev. Letters 9, 170 (1962).

[38] N. Samios, A. Bachman, R. Lea, T. Kalogeropoulos, and W. Shephard, *Proceedings of the 1962 Annual International Conference on High-Energy Physics at CERN*, edited by J. Prentki (CERN, Geneva, 1962), p. 54.

[39] See M. Roos, Rev. Mod. Phys. **35**, 314 (1963) for a detailed list of references to March 1963.